RSC Advances

PAPER

View Article Online
View Journal | View Issue

Cite this: *RSC Adv.*, 2023, **13**, 18960

Received 5th June 2023
Accepted 15th June 2023

DOI: 10.1039/d3ra03752e

rsc.li/rsc-advances

Characteristics of ignition delay of hypergolic ionic liquids combined with 1-amino-4-methylpiperazine†

Kyung Su Shin, Hoi-Gu Jang, Soon Hee Park and Sung June Cho *

The ignition delay time of the hypergolic ionic liquids, 1-ethyl-3-methylimidazolium dicyanamide [EMIM][C_2N_3] and 1,3-dimethyl imidazolium dicyandiamide [DMIM][C_2N_3], can be controlled to approximately 20 ms by adding 1-amino-4-methylpiperazine while keeping the vapor pressure below 1 torr at 298 K.

Chemical propulsion technology in the space industry using hydrazine has been considered as the state of art technology since its superior performance was proven in the 1950s.[1–3] Highly toxic hydrazine as both a monopropellant thruster with a priority catalyst and also a hypergolic bipropellant with an oxidizer such as nitrogen tetroxide and white fuming nitric acid (WFNA) has been widely utilized for a space propulsion system.[4,5] The high vapor pressure of liquid hydrazine, a major cause for high toxicity is known to be 14.2 mm_{Hg} at 298 K following the Antoine equation.[6] Also, the direct measurement of the vapor pressure of liquid hydrazine showed that the vapor pressure increased from 74.55 mm_{Hg} to 1788.88 mm_{Hg} when the temperature is raised from 324 K to 413 K. As an alternative, room temperature ionic liquids containing multiple nitrogens, as energetic ionic liquids, have been investigated extensively in order to replace toxic and hard-to-handle hydrazine or other analogs.[7–9]

It is preferable to have a short ignition delay time of less than 10 ms for aerospace applications or hypergolic propellants. However, most of the ionic liquids analyzed so far exhibit longer ignition delay times. The inclusion of fuel additives may serve as an alternative solution to reduce these delays to an acceptable range for in-space applications.[5] Dicyanamide anions have demonstrated advantageous hypergolic behavior due to their low toxicity, low viscosity, and high thermal stability.[7] Furthermore, imidazolium-based cations contribute to reducing the ignition delay time while offering additional performance benefits and physicochemical properties, making them suitable for environmentally friendly rocket propellants.[7,8,10] Thomas *et al.* demonstrated that the addition of sodium dicyanamide to 1-butyl-3-methylimidazolium dicyanamide reduced the ignition delay when used with WFNA as an oxidizer.[11] The ignition delay time depended on the additives' concentration, with a reduction of 11 ms observed when the sodium dicyanamide content was increased to 7 wt%.

Extensive research has been conducted to enhance the ignition behavior of DCA-based ionic liquids by exploring various unique additives, including graphene, graphene oxide, and boron particulates.[8,9] The ideal hypergolic additives should exhibit ignition properties similar to hydrazine and possess stability comparable to that of DCA ionic liquids. However, achieving both of these characteristics simultaneously is relatively challenging. Considering the significant potential for combining different hypergolic structures, there is a need for an efficient and systematic approach to designing high-performance hypergolic additives.

The ionic liquids, 1-ethyl-3-methylimidazolium dicyanamide [EMIM][C_2N_3] and 1,3-dimethylimidazolium dicyanamide [DMIM][C_2N_3], had the ignition delay time of 52 ms and 35 ms, respectively. However, further purification could reduce the ignition delay time, which is a critical factor in propulsion system design.

Here we report the effect of additives containing multiple nitrogens on the ignition delay time of energetic ionic liquids, [EMIM][C_2N_3] and [DMIM][C_2N_3], as shown in Scheme 1. The potential co-additives, such as diamines (including piperazine, ethylenediamine, 1,2-diaminopropane, 1,4-diaminobutane, 1-methylpiperazine, 2-methylpiperazine, 1-ethylpiperazine, 1-butylpiperazine, 1,4-dimethylpiperazine, 1-allylpiperazine, 1-amino-4-methylpiperazine [AMPZ], *etc.*), were examined by measuring the ignition delay time through drop test, as listed in

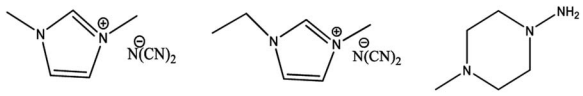

[DMIM][C_2N_3] ID=35ms | [EMIM][C_2N_3] ID=52ms | AMPZ ID=11ms

Scheme 1 Structure of energetic ionic liquids and co-additive with the measured ignition delay.

Department of Chemical Engineering, Chonnam National University, Gwangju 500-757, Korea. E-mail: sjcho@chonnam.ac.kr

† Electronic supplementary information (ESI) available. See DOI: https://doi.org/10.1039/d3ra03752e

Table 1 Ignition delay time,[a] boiling point, and corresponding vapor pressure[b] at 298 K for the co-additive compounds

Compound name	$T_{b.p.}$ (K)	P_{vap} (torr, 298 K)	ID (ms)
Ethylenediamine	389	10.4	51
1,2-Diaminopropane	392	10.6	61
1,4-Diaminobutane	432	8.0	91
1-Methylpiperazine	411	9.0	43
1-Ethylpiperazine	430	15.0	37
1-Butylpiperazine	465	9.3	44
1,4-Dimethylpiperazine	404	15.0	20
1-Allylpiperazine	454	0.7	42
1-Amino-4-methylpiperazine (AMPZ)	445	1.5	11

[a] Ignition delay time was measured through the drop test at the ambient condition when it was dropped on the oxidizer, WFNA. [b] The vapor pressure given in the table was measured triplicate using volumetric vacuum instrumentation at 298 K.

Table 1. Additionally, the vapor pressure of the corresponding compounds was compared.

The vapor pressure of the ionic liquids and AMPZ have been measured using the simple volumetric vacuum instrumentation similar to that reported earlier.[6] In brief, the liquid sample was placed in the bottle connected to the vacuum line and evacuated till 10^{-4} torr using the freeze–thaw cycle to remove the dissolved impurities such as carbon dioxide. Subsequently, the pressure increased, and vapor pressure was measured directly at 298 K after the thermal equilibrium. For [DMIM][C_2N_3] and [EMIM][C_2N_3], the obtained pressure was consistent with the reported, below 1 torr.[12] Also, the vapor pressure of 1.5 ± 0.1 torr was obtained for AMPZ, which was comparable to that of ionic liquid.

AMPZ has an ignition delay time of 11 ms, which was measured through a drop test using WFNA under ambient conditions, where a single drop of AMPZ was added to the WFNA solution.[10,13] Such a short ignition delay can be attributed to the presence of an N–N bond, like hydrazine, thereby improving the performance of the ignition delay when it is combined with the energetic ionic liquid. Thus, the combination of the results of the ignition delay time and the vapor measurement for the compound suggests that 1-amino-4-methylpiperazine is suitable for improving the hypergolic performance as a bipropellant.

[DMIM][C_2N_3] and [EMIM][C_2N_3], were each combined with AMPZ in weight percentages of 10, 20, 30, and 40 to measure the ignition delay and vapor pressure. Ignition delay time was measured in triplicate using the same method as above for AMPZ, with the ignition delay monitored using a camera with 1000 fps, allowing for 1 ms resolution in the measurement.

In Fig. 1, snapshots of the ignition delay for [DMIM][C_2N_3] and mixtures containing 20 wt% and 40 wt% AMPZ upon the contact with WFNA are presented. The ignition delay time is determined as the time interval between the initial contact of a drop with the oxidizer and the initial flash in the gas phase.[10,11,13]

As shown in Fig. 1, the ignition delay time of [DMIM][C_2N_3] was 35 ms, which is shorter than the 43 ms reported earlier for

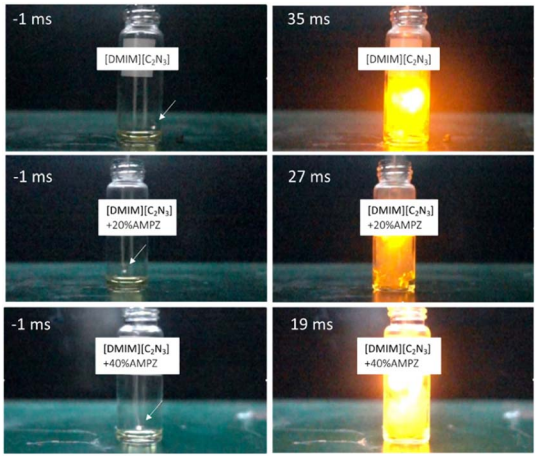

Fig. 1 Selected images at the hypergolic reaction's initial flash time when the droplet containing [DMIM][C_2N_3] combined with AMPZ was added to the WFNA. The droplet was indicated by an arrow.

other ionic liquids such as 1-butyl-3-methylimidazolium dicyanamide.[11] Indeed, the ignition delay time can vary depending on the functional group at the imidazole ring. The ignition delay of [EMIM][C_2N_3] was found to be 52 ms, significantly shorter than that reported earlier,[10] because solvent-free synthesis conditions were utilized to achieve a high yield above 95% for $[EMIM]^+$ precursor before the ion exchange of [C_2N_3], resulting in the minimization of residual solvent. The [EMIM][C_2N_3] showed a similar hypergolic reaction to that of [DMIM][C_2N_3] as shown in Fig. 1.

With an increase in AMPZ content to 40 wt% in the mixture, the hypergolic reaction of the energetic ionic liquid exhibited a decrease in ignition delay time to 20 ms (Fig. 2). The vapor pressure of the mixture was also measured triplicate and remained unchanged despite the increase in AMPZ content. Although the vapor pressure of the mixture containing AMPZ should show an increase linearly with the increase of AMPZ content, the results indicated no significant change in the vapor pressure, which suggests that AMPZ was compatible with the energetic ionic liquid. Additionally, there was no observed phase separation in the mixture even after several weeks of aging.

Further, to support the miscibility or the stability of the energetic ionic liquid and AMPZ, the DFT calculation employing CP2K package with GTH-TZV2P basis set and PBE potential was performed on 1 : 1 complex of each ionic liquid pair and AMPZ, respectively.[14] In the calculation, the total energy of the complex, ionic liquid, and AMPZ, respectively were calculated and subsequently, the stabilization energy for the aggregate was estimated following the equation below

$$\Delta E_{stabilization} = E_{T,aggregate} - E_{T,IL} - E_{T,AMPZ}$$

In the equation above, $\Delta E_{stabilization}$, $E_{T,aggregate}$, $E_{T,IL}$, and $E_{T,AMPZ}$ represent the stabilization energy, total energy for the aggregate, ionic liquid, and AMPZ, respectively after geometry

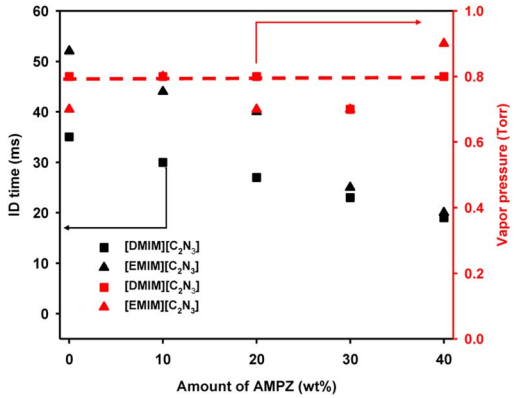

Fig. 2 The ignition delay time and vapor pressure of the mixture containing [DMIM][C_2N_3] and [EMIM][C_2N_3] with varying amounts of AMPZ are plotted as black and red symbols, respectively, in relation to the concentration of AMPZ in the mixture. The dotted line serves as a guide for the changes in vapor pressure.

optimization. The stabilization energy was found to be 0.27 eV and 0.42 eV for the complex of [DMIM][C_2N_3] or [EMIM][C_2N_3] and AMPZ, respectively. The obtained stabilization energy was comparable to that of a hydrogen bond. The optimized geometric structures for [DMIM][C_2N_3]–AMPZ and [EMIM][C_2N_3]–AMPZ are shown in Fig. 3.

The shortest distance between the N atom in the dicyanamide ion and the H atom in the methyl functional group in the imidazole ring is 2.1 Å, suggesting tight bonding in [DMIM][C_2N_3], while the shortest distance between the same atoms in [EMIM][C_2N_3] is 2.2 Å, which slightly increases, probably due to the bulky ethyl functional group.[15] When AMPZ is combined, the corresponding distance remains almost the same with a variation of only 0.1 Å. The amino group in AMPZ also appears to interact with the methyl and ethyl groups in imidazole, based on the distances of 2.3–2.4 Å from the radial distribution function, which can explain the aggregation formation energy and support the stability and miscibility of the ionic liquid and AMPZ.

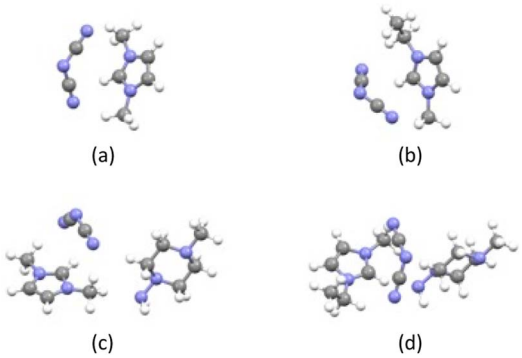

Fig. 3 The optimized structure using DFT was obtained for (a) [DMIM][C_2N_3] and (b) [EMIM][C_2N_3], and (c) and (d) for the mixture of each with AMPZ. Carbon, nitrogen, and hydrogen atoms were represented by gray, pastel blue, and white spheres, respectively.

The ESI† shows the IR spectrum of the [EMIM][C_2N_3] and AMPZ mixture as a function of AMPZ content. The IR spectrum of [EMIM][C_2N_3] remains the same with the appearance of a weak band near 2800 to 3000 cm^{-1}, which can be attributed to the increase of AMPZ due to the asymmetric C–H methyl group stretching and the symmetric stretching vibrations near 2980 cm^{-1} and 2870 cm^{-1}.[16] Additionally, the IR band at 988 cm^{-1} appears when AMPZ is mixed, which can be attributed to the non-bonding interaction of the methyl group with the amino group.

The preliminary molecular dynamics simulation was performed on the [DMIM][C_2N_3] and AMPZ aggregate in a 20 Å × 20 Å × 20 Å box using a Nose–Hoover thermostat at 373 K to ensure complete mixing for 5 ps.[17] Referring to the TG/DTA measurement under nitrogen, [DMIM][C_2N_3] and [EMIM][C_2N_3] were found to be stable up to 473 K, as shown in ESI.† The system quickly reached equilibrium, indicating the interaction between the ionic liquid and AMPZ based on kinetic energy, potential energy, and temperature. Further details can be found in ESI.† The simulation demonstrates the non-bonded interaction between the ionic liquid and the additive, AMPZ.

During the molecular dynamics simulation at 373 K, the interaction of the dicyanamide ion with the imidazolium cation can be observed by examining the distance between the terminal nitrogen in dicyanamide and the methyl functional group, as shown in ESI.†[18] The corresponding distance observed during the simulation was 2 Å, indicating that the dicyanamide ion is in close contact with the imidazolium cation.

As the dicyanamide ion moves, all hydrogens in the [DMIM][C_2N_3] molecule can interact with the dicyanamide ion for contact ion pairing. Meanwhile, the interaction between AMPZ and [DMIM][C_2N_3] can be explicitly monitored by measuring the radial distribution function between the amino group and methyl group in the imidazolium cation.[18] The corresponding radial distribution function showed that the interacting distance appeared at 2 Å, suggesting that AMPZ can diffuse in and out freely to provide homogeneous distribution in the mixture.

In summary, we find the remarkable effect of AMPZ containing hydrazine-like functional group on the reduction of the ignition delay of energetic ionic liquid around 20 ms with the low vapor pressure; otherwise, it shows a much longer ignition delay time, rendering difficulty for the design of the green propulsion system. Further, we have found the intimate interaction between AMPZ and energetic ionic liquid using DFT calculation, suggesting a compatible mixture for chemical propulsion.

Author contributions

Kyung Su Shin and Hoi-Gu Jang have contributed to the investigation and formal analysis. Hoi-Gu Jang, Soon Hee Park and Sung June Cho prepared the original draft preparation, edited, revised, and proofread the manuscript of this communication.

Conflicts of interest

There are no conflicts to declare.

Acknowledgements

This research was supported by the C1 Gas Refinery Program (2018M3D3A1A01018004) through the National Research Foundation of Korea (NRF) funded by the Ministry of Science & ICT (MSIT) and also by the Ministry of Trade, Industry, and Energy (project no. 20015736). We also thank the Pohang Acceleration Laboratory (PAL) for the synchrotron diffraction beam time.

Notes and references

1 (*a*) E. W. Schmidt, *Hydrazine and Its Derivatives*, Wiley-Interscience, New York, NY, USA, 2001; (*b*) E. Gibney, *Nature*, 2019, **566**, 434–436.

2 (*a*) G. P. Sutton, *History of Liquid Propellant Rocket Engines*, AIAA, 2012; (*b*) L. T. De Luca, *Chemical Rocket Propulsion*, Springer Nature, 2017.

3 I. J. Jang, H. S. Shin, N. R. Shin, S. H. Kim, M. J. Yu and S. J. Cho, *Catal. Today*, 2012, **185**, 198–204.

4 Y. B. Jang, T. H. Kim, M. H. Sun, J. Lee and S. J. Cho, *Catal. Today*, 2009, **14**, 196–201.

5 W.-L. Yuan, L. Zhang, G.-H. Tao, S.-L. Wang, Y. Wang, Q.-H. Zhu, G.-H. Zhang, Z. Zhang, Y. Xue, S. Qin, L. He and J. M. Shreeve, *Sci. Adv.*, 2020, **6**, eabb1899.

6 J. D. DeSain, A. G. Hsu and B. B. Brady, Aerospace Report No. TR-2018-01498, 2018.

7 (*a*) J. L. Shamshina, M. Smiglak, D. M. Drab, T. G. Parker, H. W. H. Dykes Jr, R. Di Salvo, A. J. Reich and R. D. Rogers, *Chem. Commun.*, 2010, **46**, 8965–8967; (*b*) P. D. McCrary, P. A. Beasley, O. A. Cojocaru, S. Schneider, T. W. Hawkins, J. P. L. Perez, B. W. McMahon, M. Pfeil, J. A. Boatz, S. L. Anderson, S. F. Son and R. D. Rogers, *Chem. Commun.*, 2012, **48**, 4311–4313.

8 (*a*) Q. Zhang and J. M. Shreeve, *Chem. Rev.*, 2014, **114**, 10527–10574; (*b*) R. P. Singh, R. D. Verma, D. T. Meshri and J. M. Shreeve, *Angew. Chem., Int. Ed.*, 2006, **45**, 3584–3601; (*c*) H. Gao, Y. H. Joo, B. Twamley, Z. Zhou and J. M. Shreeve, *Angew. Chem., Int. Ed.*, 2009, **48**, 2792–2795; (*d*) L. He, G. H. Tao, D. A. Parrish and J. M. Shreeve, *Chem.–Eur. J.*, 2010, **16**, 5736–5743.

9 (*a*) A. Pialat, A. A. Kitos, T. G. Witkowski, C. Cook, S. Wang, A. Hu and M. Murugesu, *New J. Chem.*, 2022, **46**, 21212–21220; (*b*) W. Zheng, X. Liu, J. Zhang, Y. Cheng and W. Wang, *Int. J. Heat Mass Transfer*, 2022, **182**, 121983; (*c*) V. N. Emel'yanenko, S. P. Verevkin and A. Heintz, *J. Am. Chem. Soc.*, 2007, **129**, 3930–3937; (*d*) P. D. McCrary, P. S. Barber, S. P. Kelley and R. D. Rogers, *Inorg. Chem.*, 2014, **53**, 4770–4776; (*e*) Y. Liu, Y. Guo, L.-H. Fei, Z. M. Mai, C. L. Tang, Z. Wang, Y. T. Wu and Z. Huang, *Energ. Mater. Front.*, 2021, **2**, 241–248.

10 J. H. Park, H. G. Jang, E. M. Goh, S. W. Baek and S. J. Cho, *Sci. Adv. Mater.*, 2017, **9**, 1863–1866.

11 A. Thomas, S. D. Chambraeau and G. L. Vaghjiani, *J. Phys. Chem. A*, 2019, **123**, 10–14.

12 (*a*) A. Berthod, M. J. Ruiz-Angel and S. Carda-Broch, *J. Chromatogr. A*, 2008, **1184**, 6–18; (*b*) O. Aschenbrenner, S. Supasitmongkol, M. Taylor and P. Styring, *Green Chem.*, 2009, **11**, 1217–1221.

13 J. Yu, S. W. Baek and S. J. Cho, *Energies*, 2019, **12**, 3208.

14 T. D. Kuehne, *et al.*, *J. Chem. Phys.*, 2020, **152**, 194103.

15 J. Hunger, S. Roy, M. Grechko and M. Bonn, *J. Phys. Chem. B*, 2019, **123**, 1831–1839.

16 M. Boumediene, B. Haddad, A. Paolone, M. A. Assenine, D. Villemin, M. Rahmouni and S. Bresson, *J. Mol. Struct.*, 2020, **1220**, 128731.

17 (*a*) S. Nosé, *Mol. Phys.*, 1984, **52**, 255–268; (*b*) W. G. Hoover, A. J. C. Ladd and B. Moran, *Phys. Rev. Lett.*, 1982, **48**, 1818–1820; (*c*) W. G. Hoover, *Phys. Rev. A*, 1985, **31**, 1695–1697.

18 (*a*) M. Brehm, M. Thomas, S. Gehrke and B. Kirchner, *J. Chem. Phys.*, 2020, **152**, 164105; (*b*) M. Brehm and B. Kirchner, *J. Chem. Inf. Model.*, 2011, **51**, 2007–2023.